无 机 化 学 学 报

2016 年　　第 32 卷　　第 1 期

目　次

论　文

基于 2-巯基苯甲酸及其原位氧化配体的两种金属配位聚合物的合成、结构及发光性质(英文)
……杨　芳　董宝霞　唐　萌　刘文龙(1)

以 1,2,4,5-苯四甲酸或 1,2,3,4-丁烷四羧酸为配体的金属有机框架的合成、表征及性质
……郭征楠　刘　峥　魏　席　唐　群　黎焕林(9)

载能碳离子撞击石墨烯中 Stone-Wales 缺陷的动力学研究
……张　超　王东琪　孟祥瑞　潘成岭　吕思远(18)

一种电荷转移晶体的磁和介电弛豫性质(英文)……张雪梅　于姗姗　张　辉　段海宝(25)

焙烧温度和掺杂浓度对 $Ca_{1-x}Sm_xWO_4$ 发光性能的影响
……吴锦绣　李　梅　柳召刚　胡艳宏　王觅堂(34)

基于 5-(4-(2,6-二(2-吡啶基)-4-吡啶基)苯氧基)间苯二甲酸的 Ni(Ⅱ)和 Cd(Ⅱ)配位聚合物的合成与晶体结构……王桂仙　曹可利　陈飞燕　冯云龙(43)

Er^{3+}/Yb^{3+}共掺杂 La_2TiO_5 荧光粉体的制备及上下转换荧光性质(英文)
……刘宣文　齐建全　郭　瑞　刘芳辰　刘　广　张晓雷　张　杨(49)

3,5-二氯水杨醛缩罗丹明 B 酰腙的合成及对 Cu^{2+}高选择性识别
……冯泳兰　方敬贤　刘　超　伍徐孟　许　猛　蒋伍玖　庾江喜　谭宇星　邝代治(56)

单分散 $Ni_xZn_{1-x}Fe_2O_4$ 纳米颗粒的制备及其磁热效应
……赵海涛　刘瑞萍　张　强　王　俏　马瑞廷(63)

$NiFe_2O_4$ 磁性纳米材料的溶剂热法一步合成
……苏碧桃　何方振　董　娜　苹俊莲　董永永　靳正娟(69)

空心结构磁性固体碱催化剂 Fe_3O_4@LDO 的制备与性能……盘登科(74)

2,6-位取代的 BODIPY 染料敏化剂的合成及其性能
……周伟男　赵鸿斌　蔡卓弟　廖俊旭　彭　飞　严文杰　阳年发(81)

不同硅铝比 Cu-ZSM-5 纳米片上 N_2O 催化分解
……邹　薇　谢鹏飞　李旭光　孔德金　华伟明　乐英红　高　滋(89)

$FeCl_3$/共轭聚席夫碱复合材料的制备及介电性能……李　俊　齐　鲁　李慧皓(96)

纳米/微米一水草酸钙、二水草酸钙对牛血清白蛋白的吸附性能
……温小玲　欧阳健明(103)

水浴法制备 CdS 薄膜产生的本征缺陷对光电学性质的影响
……徐　娜　陈　哲　索忠源　谭乃迪(111)

添加三甲基乙氧基硅烷制备耐高温硅/铝复合气凝胶
……王文琴　张志华　祖国庆　沈　军　周　斌　姚献东(117)

锂离子电池正极材料线团状 α-MnO_2 的合成及电化学性能(英文)
……徐 杉 卢 琳 刘 恋 骆义文 王石泉 刘建文 李国华 冯传启(124)
含苯并咪唑基配体钴(Ⅱ)配合物的合成、晶体结构和儿茶酚酶活性(英文)
……张 前 韩 燕 焦元红(131)
两种基于硫醇配体的银(I)配合物的合成、表征和晶体结构(英文)
……李中峰 张振伟 崔洋哲 刘 敏 杨玉平 金琼花(139)
M3 型硅酸三钙固溶体超晶胞与伪六方亚晶胞之间的取向关系及转换矩阵(英文)
……闵辉华 徐 峰 吕忆农 杨 静 丁林飞 苏 凡 朱健民(145)
2-吡啶甲醇和 1,1,1-三羟甲基乙烷混合配体七核锰配合物的合成、晶体结构与磁性(英文)
……王会生 乐 琳 潘 敏 钟文达 涂 伟 潘志权(153)
2-乙酰吡嗪缩肼基甲酸甲酯的镍和镉配合物的晶体结构及荧光性质(英文)
……毛盼东 韩学锋 吴伟娜 王冠杰 王 震 侯 莹(161)
基于 5-(3′,4′-二(四唑-5′-基)苯氧基)间苯二甲酸构筑的镧系金属配合物的合成、晶体结构及性质(英文)
……陈小莉 张潇戈 高楼军 马红燕(167)
由芳香羧酸和 1,3,5-三咪唑基苯为配体构筑的锌、镉配合物的合成、结构和荧光性质(英文)
……刘光祥(175)
两个基于 4,4′-二(1-咪唑基)苯硫醚的钴(Ⅱ)配合物的合成、晶体结构及性质(英文)
……徐 涵 郑和根(184)

《无机化学学报》投稿须知……(191)

CHINESE JOURNAL OF INORGANIC CHEMISTRY

Vol.32 No.1 Jan. 2016

CONTENTS

Cover

Magnetic and Relax-like Dielectric Response Behavior in a Charge-Transfer Crystal (English)

ZHANG Xue-Mei, YU Shan-Shan, ZHANG Hui, DUAN Hai-Bao

DOI:10.11862/CJIC.2016.002

Chinese J. Inorg. Chem., **2016**,**32**:25-33

Articles

Syntheses, Crystal Structures and Photoluminescence of Two Metal Coordination Polymers Constructed from 2-Mercaptobenzoic Acid and Its *in situ* Oxidized Ligand (English)

YANG Fang, DONG Bao-Xia, TANG Meng, LIU Wen-Long

DOI:10.11862/CJIC.2016.017

Chinese J. Inorg. Chem., **2016**,**32**:1-8

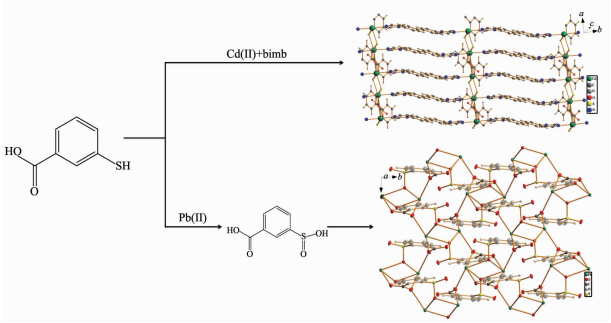

Two coordination polymers based on 2-mercaptobenzoic acid and its *in situ* oxidized ligands have been synthesized, which display 2D topological networks. The photoluminescence investigation shows that two coordination polymers appear potentially applications as new luminescent materials.

Syntheses, Characterization and Properties of Metal-Organic Frameworks based on 1,2,4,5-Benzene Tetracarboxylic Acid or 1,2,4,5-Butane Tetracarboxylic Acid

GUO Zheng-Nan, LIU Zheng, WEI Xi, TANG Qun, LI Huan-Lin

DOI:10.11862/CJIC.2016.028

Chinese J. Inorg. Chem., **2016**,**32**:9-17

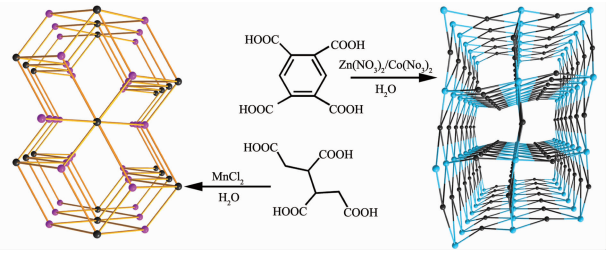

The 1,6-connected net of compound **1** and **2** is consisted of $BETA^{4-}$ ligand with five-nuclear metal clusters. The $BETA^{4-}$ ligand acts as a four-connected node, and each five-nuclear metal cluster acts as the other four-connected node. The $BTCA^{4-}$ ligand as a eight-connected node in compound **3** are linked by Mn^{2+} ions to form 4,8-connected net.

Simulation Study of Collision Dynamics of an Energetic Carbon Ion to the Stone-Wales Defect Site in Graphene

ZHANG Chao, WANG Dong-Qi,
MENG Xiang-Rui, PAN Cheng-Ling,
LÜ Si-Yuan

DOI:10.11862/CJIC.2016.025
Chinese J. Inorg. Chem., **2016**,**32**:18-24

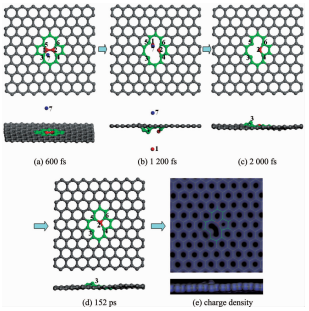

The minimum incident energy of the projectile required to drive the primary knock-on atom in the Stone-Wales defect to displace permanently from its original location is 41 eV, which is compared with the result calculated by the binary collision approximation.

Magnetic and Relax-like Dielectric Response Behavior in a Charge-Transfer Crystal (English)

ZHANG Xue-Mei, YU Shan-Shan,
ZHANG Hui, DUAN Hai-Bao

DOI:10.11862/CJIC.2016.002
Chinese J. Inorg. Chem., **2016**,**32**:25-33

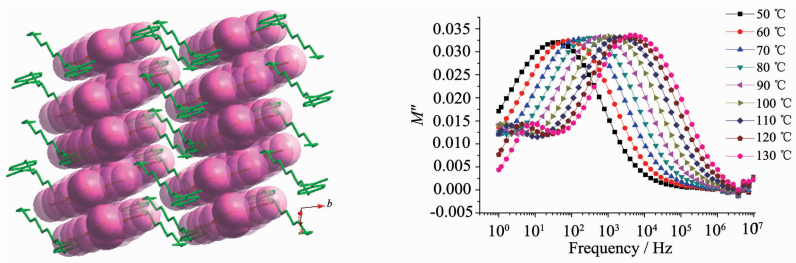

Effects of Doped Concentration and Calcination Temperature on Luminescence Properties of $Ca_{1-x}Sm_xWO_4$ Phosphors

WU Jin-Xiu, LI Mei, LIU Zhao-Gang,
HU Yan-Hong, WANG Mi-Tang

DOI:10.11862/CJIC.2016.018
Chinese J. Inorg. Chem., **2016**,**32**:34-42

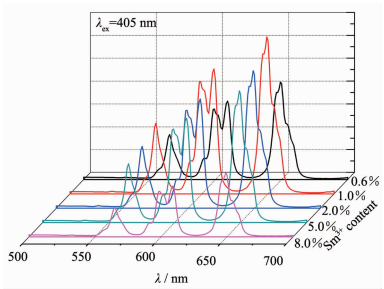

The emission spectra of $Ca_{1-x}Sm_xWO_4$ phosphors exhibit three main peaks assigned to the $^4G_{5/2}\rightarrow{}^6H_{J/2}$($J$=5, 7, 9) transitions of Sm^{3+} under 405 nm excited radiation, the dominating emission peaks at 566, 606, 650 nm. Experiments show that the best Sm^{3+} doping concentration is 1%. The energy transfer type between Sm^{3+} ions was determined to be the exchange interaction and the critical energy transfer distance (D_c) was calculated to be 2.46 nm.

Syntheses and Crystal Structures of Ni(Ⅱ) and Cd(Ⅱ) Coordination Polymers Based on 5-(4-(2,6-Di(pyrizin-2-yl) pyridin-4-yl)phenoxy)isophthalic Acid

WANG Gui-Xian, CAO Ke-Li, CHEN Fei-Yan,
FENG Yun-Long

DOI:10.11862/CJIC.2016.003
Chinese J. Inorg. Chem., **2016**,**32**:43-48

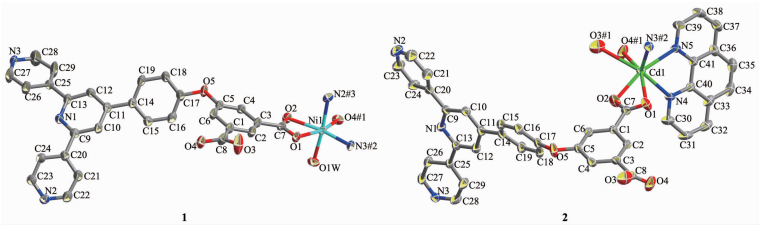

Synthesis and up/down Conversion Luminescence Properties of Er^{3+}/Yb^{3+} Co-doped La_2TiO_5 Phosphor (English)

LIU Xuan-Wen, QI Jian-Quan, GUO Rui,
LIU Fang-Chen, LIU Guang,
ZHANG Xiao-Lei, ZHANG Yang

DOI:10.11862/CJIC.2016.022
Chinese J. Inorg. Chem., **2016**,**32**:49-55

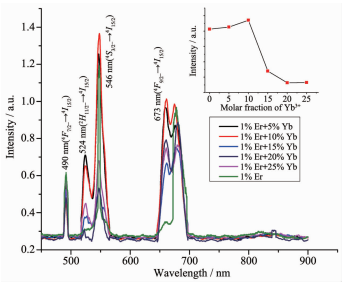

The mechanism of UC/DC luminescence of the Er^{3+} doped and Er^{3+}/Yb^{3+} co-doped La_2TiO_5 are investigated. The Yb^{3+} sensitizes effectively the UC luminescence properties of Er^{3+} and the strongest UC emission intensity is observed at 546 nm.

3,5-Dichlorosalicylaldehyde-*o*-rhodamine B Hydrazone: Synthesis and Highly Selective Recognition for Cu^{2+}

FENG Yong-Lan, FANG Jing-Xian, LIU Chao, WU Xu-Meng, XU Meng, JIANG Wu-Jiu, YU Jiang-Xi, TAN Yu-Xing, KUANG Dai-Zhi

DOI:10.11862/CJIC.2016.006
Chinese J. Inorg. Chem., **2016**,**32**:56-62

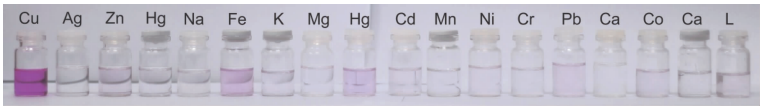

In acetonitrile/methenamine (pH 5.6) buffer system, when Cu^{2+} was added to the solution of 3,5-dichlorosalicylaldehyde-*o*-Rhodamine B hydrazone, a dramatic color change from colorless to rose red was observed, while the other metal ions did not cause noticeable changes, which indicates that 3,5-dichlorosalicylaldehyde-*o*-Rhodamine B hydrazone had a high sensitivity single selectivity colorimetric recognition for Cu^{2+}.

Synthesis and Magnetocaloric Effect of Monodisperse $Ni_xZn_{1-x}Fe_2O_4$ Nanoparticles

ZHAO Hai-Tao, LIU Rui-Ping, ZHANG Qiang, WANG Qiao, MA Rui-Ting

DOI:10.11862/CJIC.2016.015
Chinese J. Inorg. Chem., **2016**,**32**:63-68

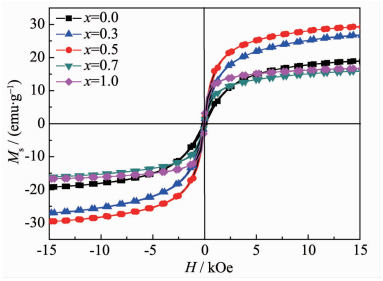

The monodisperse $Ni_xZn_{1-x}Fe_2O_4$ nanoparticles show a typical ferrimagnetic behavior at room temperature. The maximum saturation magnetization with concentration of Ni^{2+} up to x=0.5 is determined to be 29.38 emu·g^{-1}.

One-Step Synthesis of $NiFe_2O_4$ Magnetic Nanomaterial via Solvothermal Method

SU Bi-Tao, HE Fang-Zhen, DONG Na, XIN Jun-Lian, DONG Yong-Yong, JIN Zheng-Juan

DOI:10.11862/CJIC.2016.001
Chinese J. Inorg. Chem., **2016**,**32**:69-73

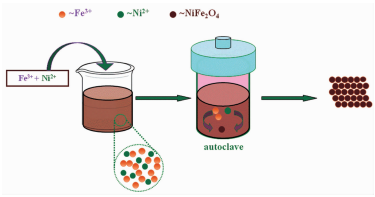

$NiFe_2O_4$ magnetic nanomaterial was prepared by one-step solvothermal method without adding any alkaline precipitation agent and high-temperature crystallization. This preparation method are of simpleness, speediness and free pollution from the source and friendly-environment.

Synthesis and Properties of the Hollow Magnetic Solid Based Catalyst Fe_3O_4@LDO

PAN Deng-Ke

DOI:10.11862/CJIC.2016.007
Chinese J. Inorg. Chem., **2016**,**32**:74-80

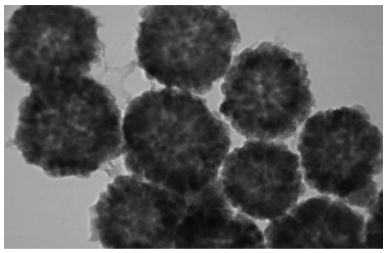

The Fe_3O_4@LDO particles possess well defined core-shell structure with Mg-Al Mixed Oxides as the shell and hollow Fe_3O_4 particle as the core, and show high catalytic activity with yield of 62% in 2 h in the Knoevenagel condensation of benzaldehyde with ethyl acetoacetate.

Synthesis and Properties of 2,6-Modified BODIPY Sensitizers for Dye-Sensitized Solar Cells

ZHOU Wei-Nan, ZHAO Hong-Bin, CAI Zhuo-Di, LIAO Jun-Xu, PENG Fei, YAN Wen-Jie, YANG Nian-Fa

DOI:10.11862/CJIC.2016.021
Chinese J. Inorg. Chem., **2016**,**32**:81-88

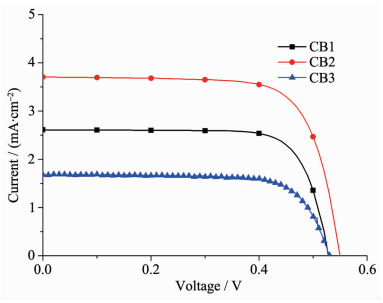

Basic optoelectronic characters and photovoltaic performances of three D-π-A type organic dye sensitizers based on BODIPY derivatives featuring BODIPY as π-conjugate bridge, N-phenylcarbazole linked BODIPY unit with different active positions as electron donor and cyanoacrylic acid as electron acceptor were systematically investigated.

Catalytic Decomposition of N_2O over Cu-ZSM-5 Nanosheets with Different n_{Si}/n_{Al}

ZOU Wei, XIE Peng-Fei, LI Xu-Guang, KONG De-Jin, HUA Wei-Ming, YUE Ying-Hong, GAO Zi

DOI:10.11862/CJIC.2016.010
Chinese J. Inorg. Chem., **2016**,**32**:89-95

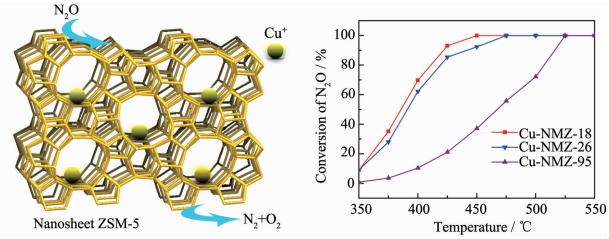

Cu-ZSM-5 nanosheets exhibit excellent activity and stability in N_2O decomposition. The catalytic activity in terms of TOF increases with the decreasing of the n_{Si}/n_{Al}, due to better reducibility of Cu^+ species and better desorption capability of adsorbed oxygen on catalysts with lower n_{Si}/n_{Al}.

Synthesis and Dielectric Properties of $FeCl_3$/Conjugated Ploy Schiff Base Composite

LI Jun, QI Lu, LI Hui-Hao

DOI:10.11862/CJIC.2016.029
Chinese J. Inorg. Chem., **2016**,**32**:96-102

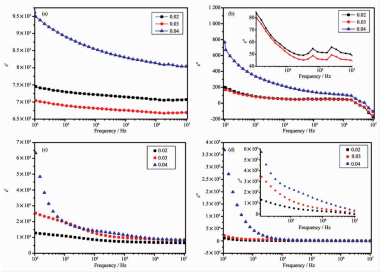

$FeCl_3$/conjugated Poly Schiff base composite with urchin-like structure was synthesized. The influence of Fe^{3+} doping content on the dielectric properties was investigated, and the optimal permittivity (ε', ε'') was achieved with 0.04 mol Fe^{3+} doped content. The permittivity of composite experienced a significant increase after 6 months.

Adsorption Properties of Bovine Serum Albumin on Micron/Nano Calcium Oxalate Monohydrate and Dihydrate Crystals

WEN Xiao-Ling, OUYANG Jian-Ming

DOI:10.11862/CJIC.2016.011
Chinese J. Inorg. Chem., **2016**,**32**:103-110

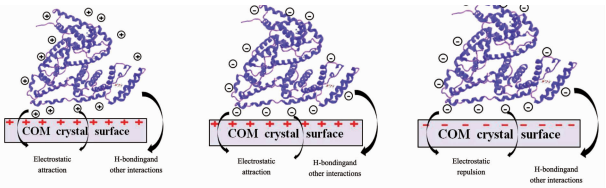

The changes of pH value changed the charged properties of crystals and BSA molecules, which affected the interactions between crystals and BSA molecules, and then affected the adsorption quantity of BSA.

Effect of Intrinsic Defects on Electrical and Optical Properties of CdS Thin Films Deposited by Chemical Bath Deposition

XU Na, CHEN Zhe, SUO Zhong-Yuan, TAN Nai-Di

DOI:10.11862/CJIC.2016.005
Chinese J. Inorg. Chem., **2016**,**32**:111-116

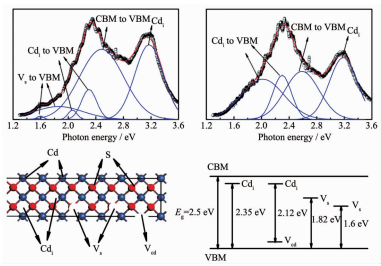

Effects of intrinsic defects such as interstitial cadmium atom (Cd_i) and sulphur vacancy (V_S) on electrical and optical properties of CdS thin films deposited at various concentration of $CdSO_4$ in solution were investigated. The decrease of donor defects (V_S) results in the reduction of conductivity and significant increase of the transmittance of CdS thin films.

Preparation of Heat-Resistant Silica/Alumina Composite Aerogel by Adding Trimethylethoxysilane

WANG Wen-Qin, ZHANG Zhi-Hua, ZU Guo-Qing, SHEN Jun, ZHOU Bin, YAO Xian-Dong

DOI:10.11862/CJIC.2016.020
Chinese J. Inorg. Chem., **2016**,**32**:117-123

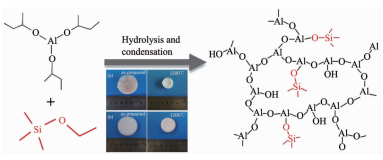

The -Si-$(CH_3)_3$ groups were introduced onto the alumina nanoparticles by adding TMEO during sol-gel process. It is demonstrated that these groups would produce SiO_2 nanoparticles, which effectively restricted the crystal growth of Al_2O_3 nanoparticles and led to the excellent heat resistance of the composite aerogels. The linear shrinkage of the obtained composite aerogel was as low as 16% and the corresponding specific surface area was as high as 141 $m^2 \cdot g^{-1}$ after heat treatment at 1 200 ℃.

Synthesis and Electrochemical Characteristics of Clew-like α-MnO_2 as Cathode Material for Lithium Ion Battery (English)

XU Shan, LU Lin, LIU Lian, LUO Yi-Wen, WANG Shi-Quan, LIU Jian-Wen, LI Guo-Hua, FENG Chuan-Qi

DOI:10.11862/CJIC.2016.013
Chinese J. Inorg. Chem., **2016**,**32**:124-130

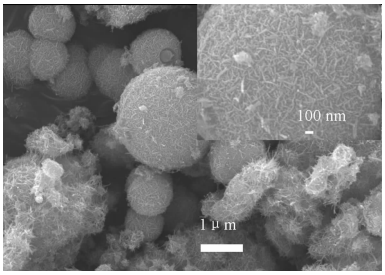

Clew-like α-MnO_2 was synthesized by a novelty synthesis method using Ag^+ as catalyst. The crystal structure, morphology and electrochemical performance of the products were characterized with the reaction temperature and reaction time as variables. The results show the product prepared at 25 ℃ for 2 days as cathode material for lithium ion battery, exhibits excellent cycling stability.

Synthesis, Crystal Structure and Catecholase Activity of the Cobalt(Ⅱ) Complex Containing Benzimidazole Ligand (English)

ZHANG Qian, HAN Yan, JIAO Yuan-Hong

DOI:10.11862/CJIC.2016.031
Chinese J. Inorg. Chem., **2016**,**32**:131-138

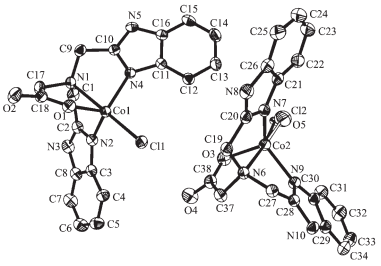

A cobalt(Ⅱ) complex showed pH value dependence for the oxidation of 3,5-di-*tert*-butylcatechol in the range of 5~11. Its catecholase catalytic activity increased with the rise of the temperature, and the kinetics obeyed the Michaelis-Menten equation.

Syntheses, Characterizations and Crystal Structures of Two Kinds of Silver(I) Complexes Derived from Thiol Ligand (English)

LI Zhong-Feng, ZHANG Zhen-Wei, CUI Yang-Zhe, LIU Min, YANG Yu-Ping, JIN Qiong-Hua

DOI:10.11862/CJIC.2016.023
Chinese J. Inorg. Chem., **2016**,**32**:139-144

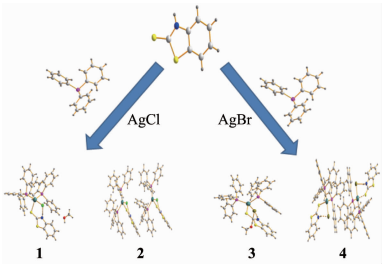

Two kinds of products were synthesized by the similar reaction condition. Single-crystal X-ray diffraction analysis reveals that **1** and **3** crystallizes in the monoclinic system with space group $P2_1/n$, while reported **2** and **4** crystallizes in the triclinic system with space group $P\bar{1}$. The luminescent spectra of the complexes show that the origin of the emissions all involves emissive state derived from ligand centered π-π* transition.

Orientation Relations and Conversion Matrix Between M3 Supercell and Pseudohexagonal Subcell in Tricalcium Silicate Solid Solution (English)

MIN Hui-Hua, XU Feng, LÜ Yi-Nong, YANG Jing, DING Lin-Fei, SU Fan, ZHU Jian-Min

DOI:10.11862/CJIC.2016.014
Chinese J. Inorg. Chem., **2016**,**32**:145-152

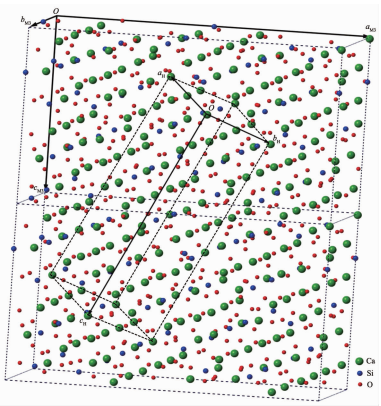

The superstructure of M3 modification in tricalcium silicate solid solution was described in detail. The orientation relations between M3 supercell and pseudohexagonal subcell was studied by computer simulation for the first time, and the conversion matrix between M3 supercell and pseudohexagonal subcell was established.

Synthesis, Crystal Structure and Magnetic Properties of a Heptanuclear Mn Complex with 2-(Hydroxymethyl) pyridine and 1,1,1-Tris (hydroxymethyl) ethane Mixed-Ligands (English)

WANG Hui-Sheng, YUE Lin, PAN Min, ZHONG Wen-Da, TU Wei, PAN Zhi-Quan

DOI:10.11862/CJIC.2016.012
Chinese J. Inorg. Chem., **2016**,**32**:153-160

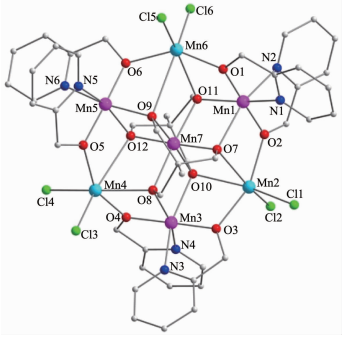

One complex containing mixed multidentate chelating ligands with different symmetry, *i.e.* $[Mn^{II}_3Mn^{III}_4(Cl)_6(hmp)_6(thme)_2]\cdot H_2O\cdot 3CH_3CN$ (**1**$\cdot H_2O\cdot 3CH_3CN$), has been synthesized and characterized. Weak frequency dependence of the ac-susceptibility for **1**$\cdot H_2O$ was found, which represents a few of examples with SMMs behavior in dislike Mn_7 clusters.

Ni(Ⅱ) and Cd(Ⅱ) Complexes with a Schiff Base Ligand Derived from 2-Acetyl Pyrazine and Methyl Hydrazinocarboxylate: Crystal Structures and Fluorescence Properties (English)

MAO Pan-Dong, HAN Xue-Feng, WU Wei-Na, WANG Guan-Jie, WANG Zhen, HOU Ying

DOI:10.11862/CJIC.2016.008
Chinese J. Inorg. Chem., **2016**,**32**:161-166

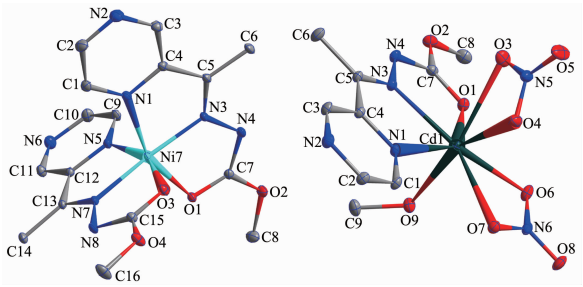

Syntheses, Crystal Structures and Properties of Two Lanthanide-Metal Complexes Based on Flexible 3′, 4′-Bis (terazol-5′-yl) phenoxy) isophthalic Acid (English)

CHEN Xiao-Li, ZHANG Xiao-Ge, GAO Lou-Jun, MA Hong-Yan

DOI:10.11862/CJIC.2016.009
Chinese J. Inorg. Chem., **2016**,**32**:167-174

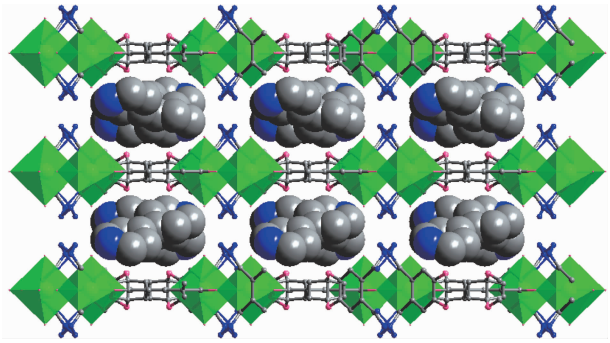

Syntheses, Crystal Structures and Luminescent Properties of Zinc(Ⅱ) and Cadmium(Ⅱ) Coordination Polymers Constructed by Aromatic Carboxylates and 1,3,5-Tris(imidazol-1-yl)benzene (English)

LIU Guang-Xiang

DOI:10.11862/CJIC.2016.024
Chinese J. Inorg. Chem., **2016**,**32**:175-183

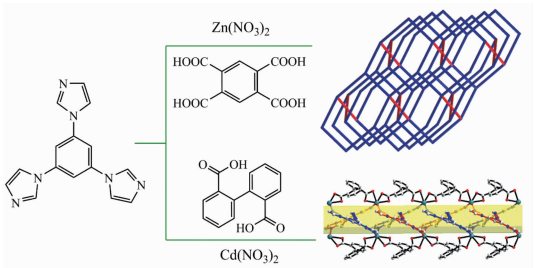

Syntheses, Crystal Structures and Properties of Two Cobalt(Ⅱ) Complexes Based on 4,4′-Bis(imidazol-l-yl)-diphenyl Thioether (English)

XU Han, ZHENG He-Gen

DOI:10.11862/CJIC.2016.016
Chinese J. Inorg. Chem., **2016**,**32**:184-190

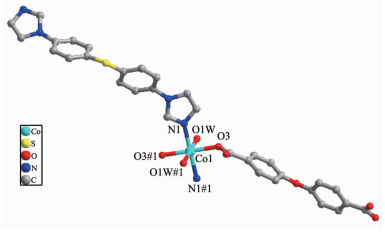

Two Cobalt coordination polymers have been synthesized and characterized by elemental analyses, IR spectra, TGA and the crystal structures were determined by single-crystal X-ray diffraction. The solid UV-Vis properties of ligands and complexes were studied at room temperature.